PHYSICS AND CHEMISTRY OF SOLID STATE
V. 19, № 1 (2018) P. 5-13
DOI: 10.15330/pcss.19.1.5-13

ФІЗИКА І ХІМІЯ ТВЕРДОГО ТІЛА
Т. 19, № 1 (2018) С. 5-13

PACS: 621.039.531

ISSN 1729-4428

M. Kondria, A. Gokhman

Isochronal Annealing of Electron-Irradiated Tungsten Modelled by CD Method: 1D and 3D Model of SIA Diffusivity

Department of Physics, South Ukrainian National Pedagogical University, Odesa-65020, Ukraine,
marianna.kondrea@gmail.com, alexander.gokhman@gmail.com

The evolution of the microstructure of tungsten under electron irradiation and post-irradiation annealing has been modeled using a multiscale approach based on Cluster Dynamics simulations. In these simulations, both self-interstitials atoms (SIA) and vacancies, carbon atoms isolated or in clusters, are considered. Isochronal annealing has been simulated in carbon free tungsten and tungsten with carbon, focusing on the recovery stages I and II. The carbon atom, single SIA, single vacancy and vacancy clusters with sizes up to four are treated as the mobile pieces. Their diffusivities as well as the energy formation and binding energies are based on the experimental data and ab initio predictions and some of these parameters have been slightly adjusted, without modifying the interaction character, on isochronal annealing experimental data. The both models with assumption on 1D as well as 3D dimensionality of diffusivity of SIA are treated. The advantage of the model with 1D diffusivity of SIA is found.

Keywords: cluster dynamics, electron irradiation, isochronal annealing, dimensional of SIA diffusivity.

Article acted received 18.01.2018; accepted for publication 05.03.2018.

Introduction

Tungsten is one of the candidate materials for the plasma facing components for fusion reactors because of its high melting point, high sputtering resistivity, and high temperature strength. Numerous studies have explored the recovery processes of radiation-induced damage in tungsten. Residual electrical resistivity was commonly used as an index of the damage present in materials for the damage recovery study, resulting in the identification of the temperatures and activation energies for different annealing stages. In this work, we gather the information available from both experimental and computational sides to clarify the dimensionality of the SIA migration in tungsten. The main point is to determine the dimensionality of the diffusivity of SIA in tungsten. The next progress could be done by Cluster Dynamics (CD) and object kinetic Monte Carlo simulations. In our paper CD is applied to simulate the kinetics of point defects in post-irradiation annealing tungsten after electron irradiation. Special attention to effect of carbon is devoted.

I. Computation model and parameteresiation.

The mean field model on the electron-irradiated and post-irradiation annealing of pure tungsten and tungsten with carbon is applied. Because the distance between point defects is expected to be much larger than dimension of the relaxation volume of point defects, the correlated recombination is not considered in our model. The single vacancies, single self-interstitial atoms (SIA_s) as well as vacancy clusters (VC) with a size up to four are considered as the mobile objects [1]. According to the data obtained by high-voltage transmission electron microscopy [2] and exhaustive kinetic Monte Carlo simulations [2,3], SIA_s in W perform 1D migration, while vacancy and VC perform 3D migration. To reveal the effect of dimensionality of SIA_s migration, the modified isotropic CD model for bcc iron with impurities [4] is applied here to study tungsten doped with carbon. Main set of parameters entering the model is presented in the Table 1.

For comparison we present here some calculated literature data: E_{bi} = 2.12eV [16]; E_{bvc} = 1.93 eV [14]; E_{bvc} =2.0eV [16]; E_{bvc} =2.39eV [17], E_{bic} =0.62eV [16], E_{bic} =0.82eV [18]. Value of surface energy, g, is taken of

Table 1

Material parameters of tungsten doped with carbon

Material parameter	Symbol	Value	Refs.
Lattice parameter	a_0	3.1652 ^{o}A	[5]
Line dislocation density	$_{d}$	10^{12} m^{-2}	[6]
Grain size	d	50μm	[5]
Burgers vector	b	2.74 ^{o}A	[5]
Capture efficiency for vacancy (SIA) by dislocation network	Z_v (Z_i)	1(1.2)	as in [4]
Recombination radius for vacancy-SIA, carbon-SIA, carbon-vacancy, (vacancy-carbon)-vacancy, (vacancy-carbon)-carbon	r_{rec}	4.65°A	as in [4,7]
Vacancy pre-exponential factors for SIA, vacancy, V_2, V_3, V_4	D_{i0}, D_{v0}, D_{2V0}, D_{3V0}, D_{3V0}	2*10^{-8} m^2/s	Assumed
Migration energy of vacancy	E_{mv}	1.5eV	[8]
Migration energy of V_2	E_{m2v}	1.6eV	Assumed
Migration energy of V_3	E_{m3v}	1.7eV	Assumed
Migration energy of V_4	E_{m4v}	1.8eV	Assumed
Migration energy of SIA	E_{mi}	0.013eV	[9]
Formation energy of SIA	E_{fi}	9.466eV	[7]
Carbon pre-exponential factor	D_{C0}	2*10^{-8} m^2/s	[10-14]
Migration energy of carbon in tungsten	E_{cm}	1.7eV	[10-14]
Surface energy		2.275 J/m^2	Estimated
Binding energy of SIA	E_{bi}	2.0 eV	Assumed
Binding energy of SIA-carbon	E_{bic}	1.15eV	Assumed
Binding energy of SIA-vacancy	E_{bvc}	2.3eV	Assumed
Binding energy of (vacancy-carbon)-vacancy	E_{bvcv}	2.3eV	Assumed
Binding energy of (vacancy-carbon)-carbon	E_{bvcc}	2.3eV	Assumed

3.119 J/m^2, which is between calculated values [15]: g = 2.275 J/m^2 for the crystallographic plane (100) and 3.221 J/m^2 for the crystallographic plane (110). In order to obtain the best agreement between CD data and experimental data [21], the migration energy of SIA is considered as a fitting parameter in our study.

II. Master Equation of Cluster Dynamics simulations.

Master Equation for both electron irradiation and post-irradiation annealing of tungsten is written by the system of ordinary differential equations for concentrations of vacancies (SIA_s) and carbon - point

defects complexes:

$$\frac{dC_{1v(i)}}{dt} = G_{dpa} - \frac{4p\ r_{rec}(D_v + D_i)C_{1v}C_{1i}}{\Omega_W} - \frac{4p\ r_{rec}(D_c + D_i)C_cC_{1iv(i)}}{\Omega_W}$$
$$- r_d Z_v \left(1 + \frac{6(r_d Z_v)^{-0.5}}{d}\right) D_{v(i)}\left(C_{1v(i)} - C^e_{1v(i)}\right) - 4\, b^{v(i)}_{1v(i)} C_{1v(i)} + 4\, a^{v(i)}_{2v(i)} C_{2v(i)} - \sum_{n=2} b^{v(i)}_{nv(i)} C_{nv}$$
$$+ \sum_{n=3} a^{v(i)}_{mv(i)} C_{nv(i)} + b^{i(v)}_{2v(i)} C_{2v(i)} - \sum_{n=2} b^{v(i)}_{ni(v)} C_{ni(v)}$$
$$- \frac{4p\ r_{rec}(D_c + D_{v(i)})}{\Omega_W} \cdot \left(C_cC_{1v(i)} - \left(C_c + C_{v(i)}\right)\exp\left(-\frac{E_{bcv(i)}}{k_BT}\right)\right) -$$
$$k_v \cdot \frac{4p\ r_{rec} D_v C_{1v} C_{vc}}{\Omega_W}\left(1 - \exp\left(-\frac{E_{bvcv}}{k_BT}\right)\right) \quad (1)$$

$$\frac{dC_{2v(i)}}{dt} = 2b^{v(i)}_{1v(i)}C_{1v} - 2a^{v(i)}_{2v(i)}C_{2v(i)} - b^{v(i)}_{2v(i)}C_{2v(i)} + a^{v(i)}_{3v(i)}C_{3v} - b^{i(v)}_{2v(i)}C_{2v} + b^{i(v)}_{3v(i)}C_{3v(i)} \quad (2)$$

$$\frac{dC_{nv(i)}}{dt} = b^{v(i)}_{(n-1)v(i)}C_{(n-1)v(i)} + \left(b^{i(v)}_{(n+1)v(i)} + a^{v(i)}_{(n+1v(i))}\right)C_{(n+1)v(i)}$$
$$- \left(b^{v(i)}_{nv(i)} + b^{i(v)}_{nv(i)} + a^{v(i)}_{nv(i)}\right)C_{nv(i)} \quad for \quad n > 2 \quad (3)$$

$$\frac{dC_{vcc}}{dt} = \frac{4p\ r_{rec} D_c}{\Omega_W} \cdot C_c \cdot C_{vc}\left(1 - \exp\left(-\frac{E_{bvcc}}{k_BT}\right)\right) \quad (4)$$

$$\frac{dC_{vcv}}{dt} = \frac{4p\ r_{rec} D_v}{\Omega_W} \cdot C_v \cdot C_{vc}\left(1 - \exp\left(-\frac{E_{bvcv}}{k_BT}\right)\right) \quad (5)$$

$$\frac{dC_{vc}}{dt} = \frac{4p\ r_{rec}(D_c + D_{v(i)})}{\Omega_W} \cdot \left(C_cC_{1v(i)} - \left(C_c + C_{v(i)}\right)\exp\left(-\frac{E_{bcv(i)}}{k_BT}\right)\right) -$$
$$\frac{4p\ r_{rec} D_v C_{1v} C_{vc}}{\Omega_W}\left(1 - \exp\left(-\frac{E_{bvcv}}{k_BT}\right)\right) -$$
$$\frac{4p\ r_{rec}(D_c + D_i)}{\Omega_W} \cdot \left(C_cC_i - \left(C_c + C_i\right)\exp\left(-\frac{E_{bic}}{k_BT}\right)\right) - \quad (6)$$

$$\frac{dC_{ic}}{dt} = \frac{4p\ r_{rec} D_c}{\Omega_W} \cdot C_c \cdot C_{vc}\left(1 - \exp\left(-\frac{E_{bvcc}}{k_BT}\right)\right) \quad (7)$$

Here G_{dpa} is electron flux, which equal to ratio of irradiation exposure (in dpa) to irradiation time for the case of electron irradiation and zero for the case of post-irradiation annealing, k_v is equal to one for vacancy and zero for SIA, $D_v(D_i) = D_{v(i)0} \cdot \exp\left(-\frac{E_{mv(i)}}{k_BT}\right)$ is the diffusivity of free vacancy (SIA), $D_c = D_{c0} \cdot \exp\left(-\frac{E_{mc(i)}}{k_BT}\right)$ is the diffusivity of free carbon atoms, $\Omega_W = \frac{a_0^3}{2}$ is the atomic volume of tungsten, $C_{1v(i)}$ is the concentration of free vacancies (SIA_s), C_c is the concentration of free carbon atoms, $C_{1v(i)e}$ is the thermal equilibrium vacancy (SIA) concentration, C_{nv} is the concentration of spherical vacancy clusters (VC) clusters contain of *n* vacancies, C_{ni} is the concentration of SIA clusters (SIAC) clusters contain of *n* SIA_s, C_{vc} and C_{ic} are the concentration of vacancy-carbon and SIA-carbon pairs , C_{vcc} and C_{vcv} are the concentration of (vacancy-carbon)-carbon and (vacancy-carbon)-vacancy complexes;

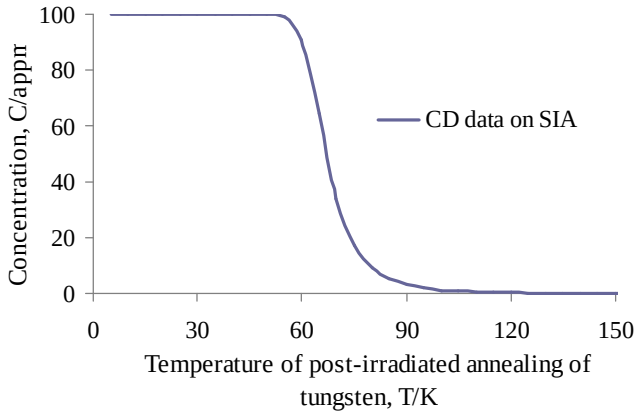

Fig. 1. Temperature dependence of concentration of free SIA in post-irradiation annealing tungsten according to CD simulations for model with 1D diffusivity of SIA.

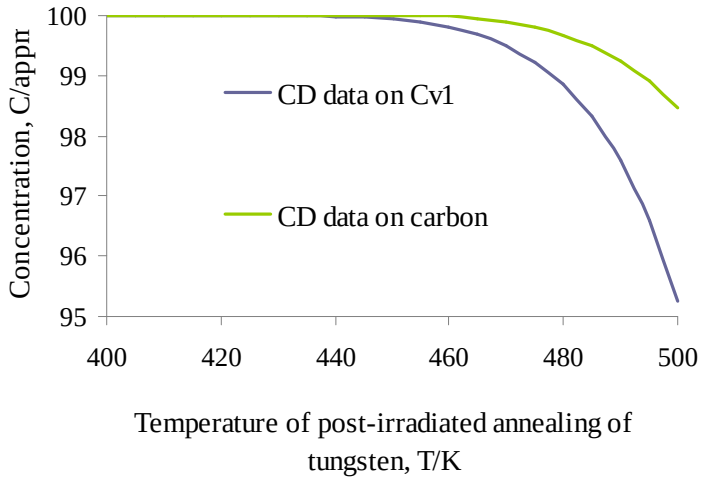

Fig. 2. Temperature dependence of concentration of free vacancies C_{1v} and free carbon C_c in post-irradiation annealing tungsten according to CD simulations for model with 1D diffusivity of SIA.

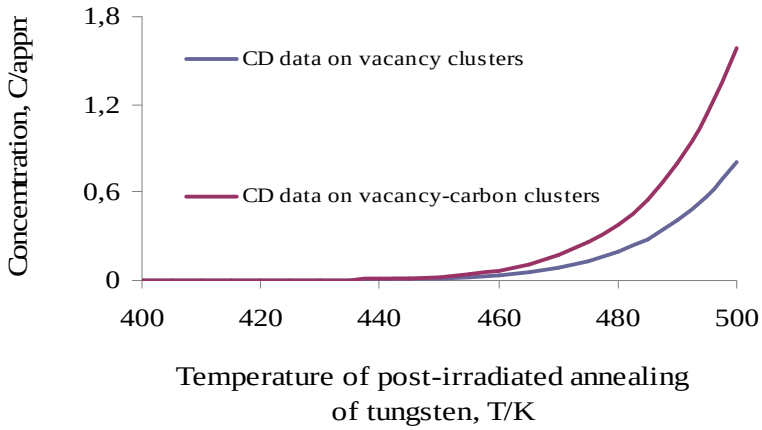

Fig. 3. Temperature dependence of concentration of vacancy clusters C_{nv} and vacancy-carbon C_{vc} pairs according to CD simulations for model with 1D diffusivity of SIA.

$b_{nv(i)}^{v(i)}$ and ($a_{mv(i)}^{v(i)}$) are the association and emission rate coefficients of vacancies V, V_2, V_3 and V_4 (SIA) from VC (SIAC), which are calculated similar to [3] and to [4] for the assumption on either 1D migration or 3D SIA migration;

1D model:

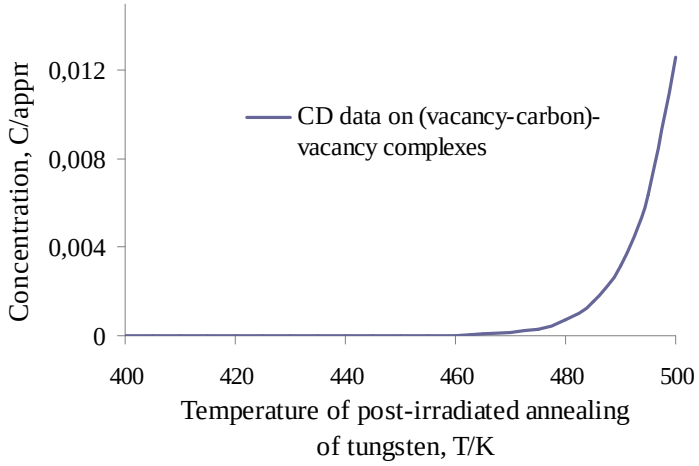

Fig. 4. Temperature dependence of concentration of (vacancy-carbon)-vacancy C_{vcc} complexes in post-irradiation annealing tungsten according to CD simulations for model with 1D diffusivity of SIA.

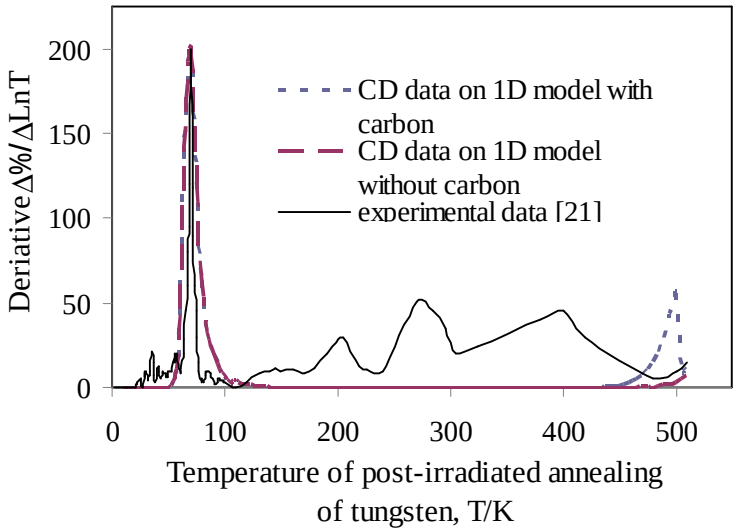

Fig. 5. Derivative versus temperature plot of the irradiation recovery data for post-irradiation annealing pure tungsten and tungsten doped with 100 appm carbon according to model with 1D diffusivity of SIA.

$b_{nv}^{v} = \frac{4p\,(r_{nv} + r_{kv})D_v C_{1v}}{\Omega}$ is the association rate coefficient of vacancy, V_2, V_3, V_4 by VC (8)

$b_{nv}^{i} = \frac{2D_i C_{1i}(p\,(r_{nv} + r_{1i}))^2 C_{nv}}{\Omega}$ is the association rate coefficient of SIA by VC (9)

$b_{ni}^{v} = \frac{2p\,(r_{ni} + r_{1v})D_v C_{1v}}{\Omega}$ is the association rate coefficient of vacancy, V_2, V_3, V_4 by SIA (10)

$b_{ni}^{i} = \frac{2D_i C_{1i}(p\,(r_{ni} + r_{1i}))^2 C_{ni}}{\Omega}$ is the association rate coefficient of SIA by SIAC (11)

$b_{ic} = \frac{2(p\,(r_i + r_c)^2)^2\ (D_i + D_c)C_c}{\Omega}$ (12)

Here, $r_{nv(i)}$ is the radius of VC (SIAC) with size of n, k=1, 2, 3, 4; r_c radius of carbon atom

3D model:

$b_{nv(i)}^{v(i)} = \frac{4p\,(r_{nv} + r_{kv(i)})D_{v(i)} C_{1v(i)}}{\Omega}$ is the attachment coefficient of vacancy, V_2, V_3, V_4 (SIA) by VC (13)

$b_{nv(i)}^{v(i)} = \frac{2p\,(r_{ni} + r_{kv(i)})D_{v(i)} C_{1v(i)}}{\Omega}$ is the attachment coefficient of vacancy, V_2, V_3, V_4 (SIA) by SIAC (14)

$b_{ic} = \frac{4p\,(r_i + r_c)(D_i + D_c)C_c}{\Omega}$ (15)

$a_{mv(i)}^{v(i)} = b_{m-1v(i)}^{v(i)} \exp\left(-\frac{E_b}{k_b T}\right)$ is the emission from cluster (16)

The system of Equations (1-16) describes:

(1) generation of free vacancy and SIA due electron irradiation;

(2) vacancy - SIA recombination;

(3) sinking of vacancy (SIA) at dislocation network;

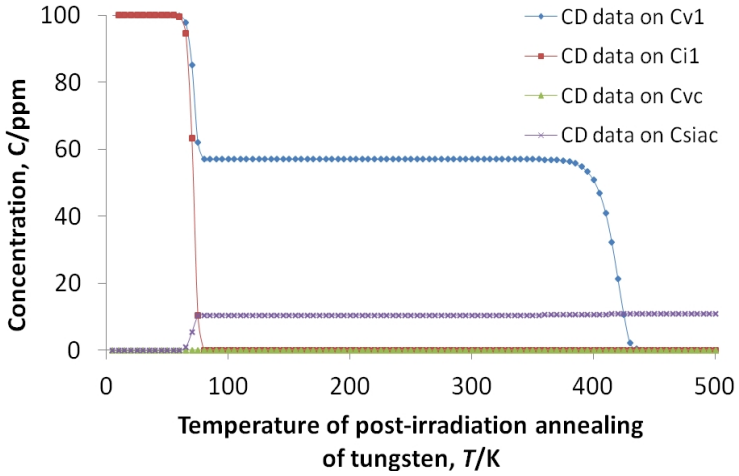

Fig. 6. Temperature dependence of concentration of free vacancies (C_{1v}), free SIA_s (C_{1i}), clustering vacancies into VC (C_{nv}) and clustering SIA into SIAC (C_{ni}) in post-irradiation annealing tungsten doped with 100 appm carbon according to the model with 3D diffusivity of SIA.

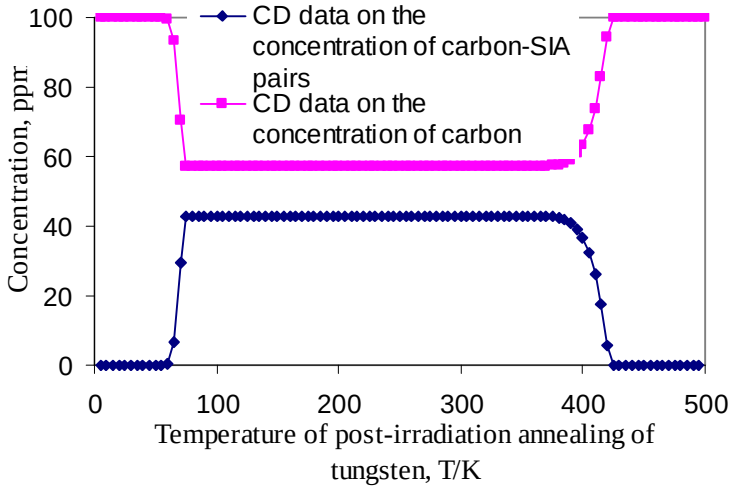

Fig. 7. Temperature dependence of concentration of SIA-carbon pairs C_{ic} and carbon C_c in post-irradiation annealing tungsten doped with 100 appm carbon according to the model with 3D diffusivity of SIA.

(4) trapping of vacancy (SIA) by carbon;

(5) absorption of vacancy (SIA) by VC) and SIAC;

(6) emission of vacancy and SIA from VC and SIAC, respectively;

(7) absorption (emission) of VC with two, three and four vacancies by (from) VC;

(8) absorption (emission) of carbon or vacancy by (from) vacancy-carbon complex.

III. Cluster Dynamics simulations.

Because the evolution of point defect system in post-irradiation annealed tungsten is the set of kinetics processes with the different characteristic times, the integration of the Master Equation (1-17) is the typical problem of stiff ordinary differential equations. Stiff equation is a differential equation for which classical numerical methods for solving the equation are numerically unstable, unless the step size is taken to be extremely small. Hence, the FORTRAN subroutine package, *LSODE*, the Livermore Solver for Ordinary Differential Equations [19] based on the backward differentiation formula method [20] has been taken as a main program of computer code. Following to [21], the electron irradiation exposure, irradiation time and irradiation temperature are taken as 0.0001 dpa, 43200 seconds and 5 K; the temperature step of isochronal annealing is taken to be 5 K, the annealing time on every step is 300 seconds below 450 K and 600 seconds in the range 450 K to 500 K. CD simulations have been done for the initial concentration of free carbon atoms in tungsten about 100 appm and for tungsten free from carbon. To compare CD results with experimental measurements [21], the differential isochronal resistivity recovery has been calculated according to [21,22]:

$$100\% \frac{(r-r_0)/r_0}{LnT-LnT_0} = 100\% \frac{(n-n_0)/n_0}{LnT-LnT_0} \qquad (17)$$

Here r and r_0 are the specific electrical resistivity for given temperature T and the residual resistivity, respectively; n and n_0 are the total number of Frenkel pairs at temperatures T and T_0.

Model implies the 1D migration of SIA.

It was found that electron irradiation of 0.0001 dpa during 43200 seconds at temperature of 5 K results in generation of Frenkel pairs with concentration about 100 ppm in both pure tungsten and tungsten doped with carbon. The value of E_{mi} about 0.125eV provided the best fit of CD simulation to the experimental data [21]. Calculated by CD temperature dependences of concentration of free SIA, free vacancies, free carbon atoms, vacancy clusters, vacancy-carbon clusters and (vacancy-carbon)-vacancy complexes in the post-irradiation annealed tungsten are presented on Fig. (1-4). Concentration of SIA_s decreases from 100 appm to zero due to the annealing in the temperature diapason (55; 105) K (Fig.1). Concentration of free vacancies (C_{v1}) and free carbon atoms (C_{carbon}) is about of 100 appm in the temperature diapason (5; 450) K; next increase of the annealing temperature in the diapason (450; 500) K results in the slight decrease of the concentration of C_{v1} and C_{carbon} (Fig. 2). Vacancy clusters, vacancy-carbon pairs and vacancy-carbon-vacancy complexes start to form in the mentioned temperature diapason (Fig. 3,4).

The calculated differential isochronal resistivity recovery curves for both pure tungsten and carbon-doped tungsten are presented on Fig. 5. The complete agreement of the calculated and experimental position and amplitude of the recovery peak in the temperature diapason from 5 to 100 K (Stage I) was found. Some agreement of the experimental and calculated recovery spectrum is observed at the end of Stage II (100; 500) K.

Model implies the 3D migration of SIA.

As well as for the model on 1D diffusivity of SIA, it was found that electron irradiation of 0.0001 dpa during 43200 seconds at temperature of 5 K results in generation of Frenkel pairs with concentration about 100 appm in both pure tungsten and tungsten with carbon. The value of E_{mi} about 0.163eV provided the quite good coincidence on the experimental position of first recovery peak [21] and simulation data. Calculated by CD temperature dependences of concentration of free and clustering vacancies and SIA_s; free carbon atoms, vacancy-carbon, SIA-carbon, VC-V and VC-V complexes in the post-irradiation annealed tungsten doped with carbon are presented on Fig. (6,7).

For the temperature range of isochronal annealing from 4.2 to 100 K (Stage I of the recover spectrum of tungsten [21]), we observe:

1) decrease of the concentration of free vacancies to value about 29 ppm (57 ppm) for pure tungsten (tungsten with carbon) and of free SIA to zero for both pure tungsten (tungsten with carbon), formation of SIA clusters (SIAC) with concentration of SIA in clusters about 21 ppm (10.6 ppm) for pure tungsten (tungsten with carbon), no VC formation for both pure tungsten (tungsten with carbon) in the temperature range from 55 to 100 K;

2) formation of SIA-carbon pairs with concentration about 43 ppm and decrease of free carbon atoms to value about 57 ppm for tungsten with carbon at the end of first stage;

3) no formation of vacancy-carbon, (vacancy-carbon)-vacancy and (vacancy-carbon)-carbon.

For the temperature range of isochronal annealing from 100 to 500 K (Stage II of the recover spectrum [21]), we observe:

(1) decrease of the concentration of free vacancies to zero, no significant changes of concentration of free SIA, formation of vacancy-carbon and SIA-carbon pairs in the temperature range from 360 to 500 K;

(2) decrease of the concentration of SIA-carbon pairs to zero, increase of concentration of carbon atoms to 100 appm, for the tungsten with carbon in the same temperature range;

(3) no significance change of concentrations of point defects for pure tungsten;

(4) very low concentration of vacancy-carbon, (vacancy-carbon)-vacancy and (vacancy-carbon)-carbon.

The calculated differential isochronal resistivity recovery is presented on Figure 8.

Model on 3D diffusivity of SIA reproduces in CD simulations the position of experimental recovery peak at the Stage I centered about 70 K for both pure tungsten

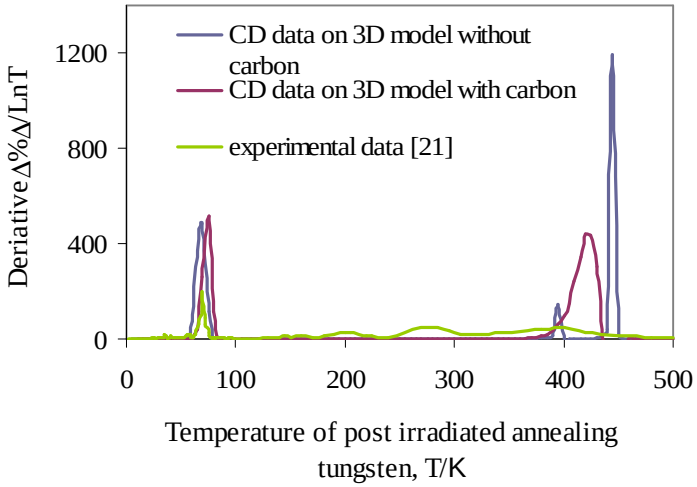

Fig. 8. Derivative versus temperature plot of the irradiation recovery data for post-irradiation annealing pure tungsten and tungsten with 100 ppm carbon according to model with 3D diffusivity of SIA.

and tungsten doped with carbon but calculated amplitude (about of 500) more large than experimental one (about of 200). Moreover, the calculated recovery peaks at the end of the Stage II are not observed in experiment [21].

IV. Discussion

The position of the first experimental peak of differential isochronal resistivity recovery of tungsten [21] is reproduced well by the CD simulations according to both models with 1D and 3D SIA migration. The 1D diffusion model provides the complete agreement of the calculated and experimentally-measured amplitude of the first recovery peak. While the 3D diffusion model overestimates the amplitude of the peak by a factor of two compared to the experimental value. The addition of carbon up to 100 appm has no influence on the calculated position and amplitude on the first recovery peak. Similar effect is found by atomistic kinetic Monte Carlo simulations in [22], where the effect of the copper on the recovering spectrum of electron irradiated Fe-Cu alloys has been investigated. To achieve the best agreement between CD simulations and experimental data [21] the value of E_{mi} of 0.125eV has been taken in CD simulations according to 1D model diffusivity of SIA. It is less than E_{mi} of 0.163eV found for 3D model of diffusivity but far from E_{mi} of 0.013eV calculated in [9]. Hence, the value of SIA migration energy of 0.125eV could be considered as the effective one. The reason of the divergence this value from data [9] can be the use of mean field model in CD simulations while 1D migration of SIA is spatially correlated [2].

CD simulations result in the strong peak of the recovery spectrum at the end of Stage II for model with 3D diffusivity of SIA but this peak isn't observed in experiment [21]. Contrary, there is a set small recovery peaks are observed experimentally in this temperature range [21]. Note, this regularity isn't common for recovery of irradiated materials, where only one peak is on the each recovery stage (look, for example, [23]. The paucity of experimental data points in any apparent peaks for the Stage II mentioned by authors of [21] points out on the necessity to carry out the additional study of this stage by resistivity recovery as well as by positron annihiliation spectroscopy and other methods. CD model with 1D diffusivity of SIA result in some coincidence of the experimental [21] and calculated recovery spectrum at the end of Stage II.

Conclusion

The comparison of CD results for the models with 1D diffusivity and 3D diffusivity of SIA with experimental data on isochronal annealing of electron-irradiated tungsten in tungsten [21] supports the statement of the density functional theory simulations [7], TEM study [2] and kinetic Monte Carlo simulations [2,3] on the 1D diffusivity and consequently crowdion structure of SIA in tungsten.

Kondria M.S. — PhD student of Department of Physics;
Gokhman O.R. — Dc. of Sci. in Physics of Metals, Prof. of Department of Physics, Head of Department of Physics.

[1] C.C. Fu, J. Dalla Torre, F. Willaime, J.L. Bocquet and A. Barbu, Nature Materials (4), 68 (2005).
[2] T. Amino, K. Arakawa & H. Mori, , Scientific Reports | 6:26099 | DOI: 10.1038/srep26099 (2016).
[3] N. Castin, A. Bakaev, G. Bonny, A. E. Sand, L. Malerba, D. Terentyev, Journal of nuclear materials (1), 15 (2018).
[4] A. Gokhman, S. Pecko and V. Slugeň, Radiation Effects and Defects in Solids: Incorporating Plasma Science and Plasma Technology (170), 745 (2015).
[5] J. Fikar and R. Schaublin. Nucl. Instr. Methods Phys. Res. B (267), 32.18 (2009).
[6] G. E. Dieter. Mechanical Metallurgy. McGraw-Hill Book Company, London, symmetric edition (1988).
[7] Y. G. Li, W. H. Zhou, R. H. Ning, L. F. Huang, Z. Zeng1, X. Ju, Commun. Comput**.** Phys. (11), 1547 (2012).
[8] A. Satta, F. Willaime, and Stefano de Gironcoli, Phys. Rev. (B 57), 11184 (1998).
[9] P. M. Derlet, D. Nguyen-Manh, and S. L. Dudarev, Phys. Rev.(B 76), 054107 (2007).
[10] Withop, Arthur, PhD Thesis, The diffusion of carbon into tungsten, The University of Arizona, (1966).
[11] L.N. Aleksandrov, Zavodskaya Laboratorly (25), 925 (I960).
[12] Becker, J. A., E. I. Becker, and Re. G. Brandes, J. Appl. Phys. (32), 411 (1961).
[13] C. P. Bushmer, P. H., Journal of Material Science (6), 981 (1971).
[14] Yue-Lin Liu, Hong-Bo Zhou, Shuo Jin, Ying Zhang and Guang-Hong Lu, J. Phys.: Condens. Matter (22), 445504 (2010).
[15] W.R. Tyson, W.A. Miller, Surface Science (62), 267 (1977).
[16] C.S. Becquart, C. Domain, U. Sarkar, and et al., J. Nucl. Mater., (403), 75 (2010).
[17] D. Nguyen-Manh, Advanced Materials Research (59), 253 (2009).
[18] Xiang-Shan Kong, Xuebang Wua, Yu-Wei You, C.S. Liu, Q.F. Fang, Jun-Ling Chen, G.-N. Luo, Acta Materialia (66), 172 (2014).
[19] LSODA is part of the ODEPACK provided by Alan C. Hindmarsh 1984 on the CASC server of the Lawrence Livermore National Laboratory, Livermore, CA 94551, USA.
[20] Gear,: Numerical Initial Value Problems in Ordinary Differential Equations. Prentice-Hall, Englewood Cliffs, NJ, 1971.
[21] H.H. Neely, D.W. Keeper and A. Sosin, Phys. stat. sol. (28), 675 (1968)

М.С. Кондря, О. Р. Гохман

Ізохронний відпал електронно-опроміненого вольфраму, моделювання за методом кластерної динаміки: 1D та 3D модель дифузії міжвузельного атому

Південноукраїнський національний педагогічний університет імені К.Д. Ушинського, вул. Старопортофранківська, 26, м. Одеса, 65020, Україна, marianna.kondrea@gmail.com, alexander.gokhman@gmail.com

Еволюція мікроструктури вольфраму під впливом електронного опромінення та пост-опроміненого відпалу була змодельована з використанням мультімасштабного підходу, який базується на використанні методу кластерної динаміки. Розглядається кінетика кластерів вакансії, міжвузельних атомів та атомів вуглецю. Проводиться моделювання формування дефектної структури вольфраму без вуглецю і вольфраму з вуглецем під дією пост-опроміненого ізохронного відпалу на його I і II стадіях. Вакансійні кластери з розміром до чотирьох вакансій, міжвузельні атоми та атоми вуглецю розглядаються як рухомі об’єкти. Вибір у дослідженні значень коефіцієнтів дифузії, енергії формування дефектів, енергії їх зв'язків грунтується на експериментальних даних або результатів розрахунків ab-initio. Деякі параметри додатково коректуються з метою досягнення кращої згоди даних моделювання та даних вимірювання електричного опіру при ізохронному відпалі. Розглядаються моделі з припущенням про різну вимірність дифузії міжвузельного атому. Показано перевагу моделі з припущенням про 1D дифузію міжвузельного атому.

Ключові слова: кластерна динаміка, електронне опромінення, ізохронний відпал, розмірність дифузії міжвузельного атому.